

PPPL- 5120

PPPL-5120

## The Joint Influence of Albedo and Insulation on Roof Performance: An Observational Study

P. Ramamurthy, T. Sun, K. Rule, and E. Bou-Zeid

February 2015



Prepared for the U.S. Department of Energy under Contract DE-AC02-09CH11466.

# Princeton Plasma Physics Laboratory

## Report Disclaimers

---

### Full Legal Disclaimer

This report was prepared as an account of work sponsored by an agency of the United States Government. Neither the United States Government nor any agency thereof, nor any of their employees, nor any of their contractors, subcontractors or their employees, makes any warranty, express or implied, or assumes any legal liability or responsibility for the accuracy, completeness, or any third party's use or the results of such use of any information, apparatus, product, or process disclosed, or represents that its use would not infringe privately owned rights. Reference herein to any specific commercial product, process, or service by trade name, trademark, manufacturer, or otherwise, does not necessarily constitute or imply its endorsement, recommendation, or favoring by the United States Government or any agency thereof or its contractors or subcontractors. The views and opinions of authors expressed herein do not necessarily state or reflect those of the United States Government or any agency thereof.

### Trademark Disclaimer

Reference herein to any specific commercial product, process, or service by trade name, trademark, manufacturer, or otherwise, does not necessarily constitute or imply its endorsement, recommendation, or favoring by the United States Government or any agency thereof or its contractors or subcontractors.

---

## PPPL Report Availability

### Princeton Plasma Physics Laboratory:

<http://www.pppl.gov/techreports.cfm>

### Office of Scientific and Technical Information (OSTI):

<http://www.osti.gov/scitech/>

---

### Related Links:

[U.S. Department of Energy](#)

[Office of Scientific and Technical Information](#)

## Accepted Manuscript

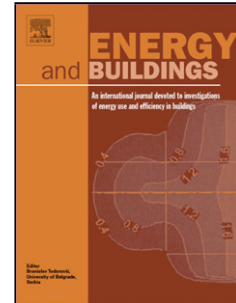
Title: The Joint Influence of Albedo and Insulation on Roof Performance: An Observational Study

Author: P. Ramamurthy T. Sun K. Rule E. Bou-Zeid

PII: S0378-7788(15)00145-0  
DOI: <http://dx.doi.org/doi:10.1016/j.enbuild.2015.02.040>  
Reference: ENB 5714

To appear in: *ENB*

Received date: 17-12-2014  
Revised date: 14-2-2015  
Accepted date: 16-2-2015



Please cite this article as: P. Ramamurthy, T. Sun, K. Rule, E. Bou-Zeid, The Joint Influence of Albedo and Insulation on Roof Performance: An Observational Study, *Energy and Buildings* (2015), <http://dx.doi.org/10.1016/j.enbuild.2015.02.040>

This is a PDF file of an unedited manuscript that has been accepted for publication. As a service to our customers we are providing this early version of the manuscript. The manuscript will undergo copyediting, typesetting, and review of the resulting proof before it is published in its final form. Please note that during the production process errors may be discovered which could affect the content, and all legal disclaimers that apply to the journal pertain.

# **The Joint Influence of Albedo and Insulation on Roof Performance: An Observational Study**

**P. Ramamurthy<sup>1,2</sup>, T. Sun<sup>3</sup>, K. Rule<sup>4</sup> and E. Bou-Zeid<sup>2\*</sup>**

1-Department of Mechanical Engineering, The City College of New York, New York, NY 10031.

2-Department of Civil and Environmental Engineering, Princeton University, Princeton NJ 08544.

3- Department of Hydraulic Engineering, Tsinghua University, Beijing 100084, China

4-Princeton Plasma Physics Laboratory, Princeton NJ 08540.

\* *Corresponding Author: Princeton University Department of Civil & Environmental Engineering E414, EQuad*

*Princeton, NJ 08544 USA Tel: +1-609-258-5429 email: ebouzeid@princeton.edu*

## **Abstract**

This article focuses on understanding the temperature and heat flux fields in building roofs, and how they are modulated by the interacting influences of albedo and insulation at annual, seasonal and diurnal scales. High precision heat flux plates and thermocouples were installed over multiple rooftops of varying insulation thickness and albedo in the Northeastern United States to monitor the temperature and the heat flux into and out of the roof structures for a whole year. Our analysis shows that while membrane reflectivity (albedo) plays a dominant role in reducing the heat conducted inward through the roof structures during the warmer months, insulation thickness becomes the main roof attribute in preventing heat loss from the buildings during colder months. On a diurnal scale, the thermal state of the white roof structures fluctuated little compared to black roof structures; membrane temperature over white roofs ranged between 10°C and 45°C during summer months compared to black membranes that ranged between 10°C and 80°C. Insulation thickness, apart from reducing the heat conducted through the roof structure, also delayed the transfer of heat, owing to the thermal inertia of the insulation layer. This has important implications for determining the peak heating and cooling times.

25 **Keywords**

26 Cool Roof, Roof albedo, Roof heat flux, Roof insulation

27 **1 Introduction**

28 According to a recent report by the US Department Of Energy[1], the US buildings sector  
29 accounted for nearly 41% of national primary energy consumption (i.e. about 7% of the primary  
30 energy consumption of the whole world) and almost half of this fraction was used for space  
31 heating/cooling. These numbers underline the large share of worldwide energy that is consumed  
32 for building air conditioning and suggest that even moderate savings in building energy  
33 consumption could go a long way in advancing the world towards future energy sustainability.

34 Given their large contribution to total building heating and cooling energy consumption [1], [2],  
35 roofs are increasingly the focus of current research and development efforts. Newer concepts in  
36 roof design such as cool (highly reflective) roofs [3], [4], [5] and green roofs [6] are being  
37 explored by various researchers. These designs, apart from improving the energy efficiency of  
38 the buildings, would also have a significant impact on the urban microclimate when implemented  
39 at a sufficiently large scale over a given city [7]. While these efforts have underlined the  
40 importance of roofs and the potential of their retrofits in decreasing building energy consumption  
41 and improving the urban microclimate at various locations, few studies have (a) included  
42 measurements inside the roof insulation layers to understand the effect of the roofs' thermal  
43 inertia, (b) combined measurement and modeling methodologies with thorough model validation  
44 at multiple levels, or (c) examined in-depth the interacting roles of roof albedo (averaged  
45 reflectivity) and insulation thickness in reducing heat fluxes through the roof structure. In  
46 addition, many studies treat roof structures as homogeneous entities with fixed physical and  
47 thermal properties [8]. But real-roofs are composed of membranes, insulators, decks and other

48 elements, each with their own unique attributes. These simplified approaches, while adequate to  
49 provide estimates of the impact of certain roof designs on building energy efficiency, are not  
50 suitable for probing the thermal dynamics in complex, vertically-heterogeneous, roof structures,  
51 or for asserting how local climatology influences optimal roof design.

52 One consequence of the residual knowledge gap for example is that for large parts of the US,  
53 there are yet no clear and conclusive recommendations as to whether white or black roof are  
54 more efficient over the course of whole year. As such, there is clearly much that remains to be  
55 learned about the thermal dynamics in roof layers and how they affect building performance.  
56 Furthermore, there is urgency in filling these knowledge gaps in light of the increasing attention  
57 given recently to building energy savings. In the US for example, the Department of Energy has  
58 recently created through a \$120 million grant the “Energy Efficient Buildings Hub”  
59 (<http://www.eebhub.org>); this work is in fact, and for full-disclosure, part of a project funded by  
60 that hub.

61 A number of recent studies have focused on retrofitting old buildings with newer roofs that have  
62 a higher reflectivity membrane and a sound insulation layer [9]-[12]. The modern roof structures  
63 used in such retrofits or in new buildings typically consist of a membrane on top, one or more  
64 insulation layers (plywood, fiber board, PolyIso (polyisocyanurate), polystyrene foam)  
65 underneath, and a concrete or steel roof deck at the bottom. All these materials have varying  
66 physical and thermodynamic properties that modulate heat transfer through the roof. The  
67 membranes are usually thinner and are coated either black or white, which directly affects the  
68 albedo [1], [13]. The insulation layer beneath the membranes has low thermal conductivity [3],  
69 [4], [14] and low heat capacity, enabling it to reduce the transfer of heat to/from the building and  
70 also extending the life of the membrane layer above it. The insulation layers, apart from

71 restricting the transfer of heat by means of low thermal conductivity  $k$  ( $\text{W m}^{-1} \text{K}^{-1}$ ), also delay  
72 the transfer towards the indoor space due to their thermal inertia or effusivity  $(k \rho c)^{1/2}$ , where  $\rho$   
73 ( $\text{kg m}^{-3}$ ) is the insulation material density and  $c$  ( $\text{J K}^{-1} \text{kg}^{-1}$ ) is the specific heat capacity. The  
74 thermal effusivity is a measure of a materials ability to exchange thermal energy with its  
75 surroundings. While the inherent thermal properties restrict the transfer of heat/cold in/out of the  
76 buildings, aging reduces the thermal efficiency of the membranes and insulation foams. Natural  
77 weathering and accumulation of dust particles decrease the albedo of cool roof membranes [5],  
78 [15], [16] and the inert gas that occupies the cell structure of most PolyIso foams diffuses out and  
79 gets replaced by air, thereby increasing the foams thermal conductivity and reducing its heat  
80 transfer resistivity [6], [17], [18]. These effects, combined with the heterogeneous roof  
81 structures, complicate sensing and modeling of such roofs.

82 In this paper, our focus is on experimentally investigating roof structures as heterogeneous  
83 entities to elucidate the effects of thermal inertia and albedo on their efficiency in regulating heat  
84 transfer into buildings. Of particular interest is the covariance of the effects related to these two  
85 roofs parameters: insulation thickness and albedo. To accomplish these aims, we will analyze  
86 heat flux and temperature observations at various levels inside different roof elements, and  
87 combine them with measurements of atmospheric forcings to study the performance of roof  
88 structures.

89

## 90 **2 Methodology**

91 The test site for this study was the Princeton Plasma Physics Lab (PPPL) in Princeton, New Jersey,  
92 USA (N 40.3489° W74.6029°). PPPL consists of a block of interconnected buildings of various  
93 heights, built during different time periods. The naming convention, building's respective age, and

94 the roof heights above ground level (AGL) are detailed in Table 1. The table also gives the R-  
 95 value, which is a measure of the total thermal resistance of the roof insulation:  $R = d / k$ , where  $d$  is  
 96 the insulation depth and  $k$  is the thermal conductivity of the roof. The SI unit of  $R$  is  $\text{m}^2 \text{K W}^{-1}$ ; the  
 97 table also lists (within braces) the R-value in the more commonly used units in the US, which is  
 98  $\text{hr ft}^2 \text{ }^\circ\text{F BTU}^{-1}$ . Note that the SI R-value ( $\text{m}^2 \text{K W}^{-1}$ ) = 5.71 R-value ( $\text{hr ft}^2 \text{ }^\circ\text{F BTU}^{-1}$ ).

99 Table 1: Building and Roof information.

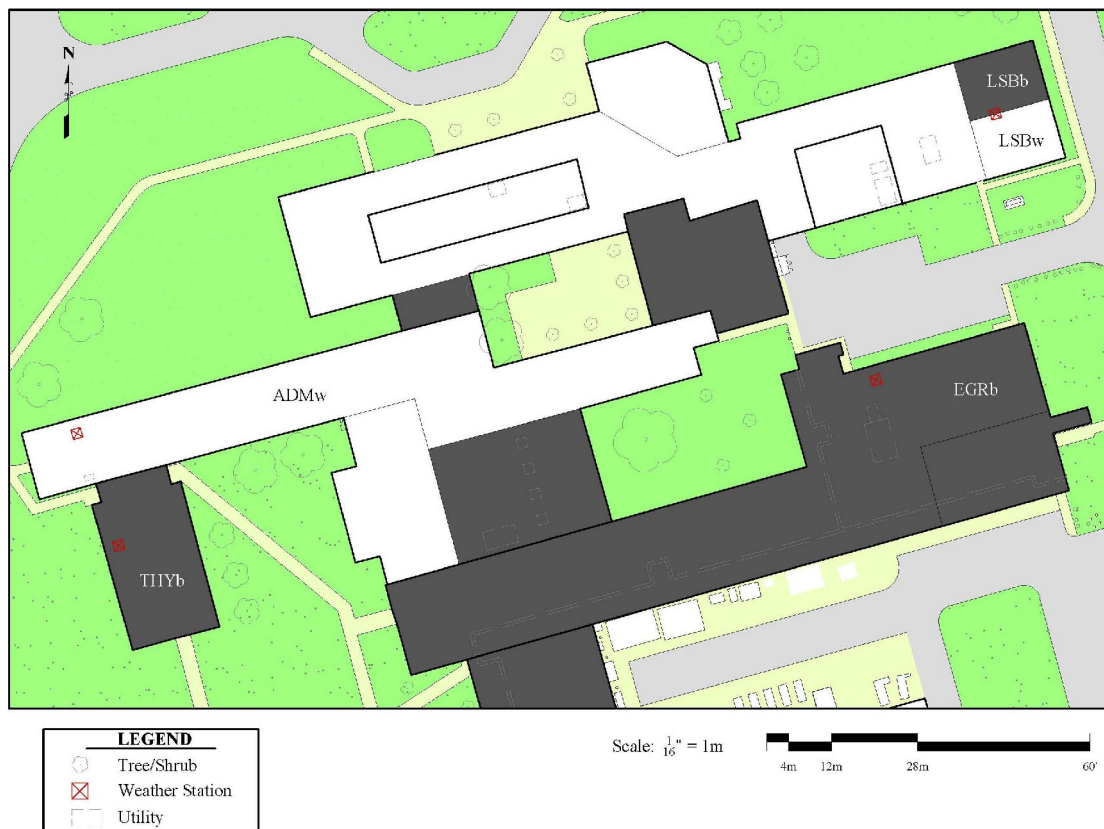
<b>Building name /Rooftop elevation</b>	<b>Year of Construction</b>	<b>Roof color, R-value (<math>\text{m}^2 \text{K W}^{-1}</math>) at sensor location, year of last retrofit</b>
Admin (ADMw-R8.4) (3.3 m AGL)	1962	White, R8.4 (US unit R48), 2005
Theory (THYb-R3.7) (3.18 m AGL)	1978	Black, R3.7 (US unit R21), 2002
Lyman Spitzer (LSBb-R4.2) (13.38 m AGL)	1992	Black, R4.2 (US unit R24), 2012
Lyman Spitzer (LSBw-R4.2) (13.38 m AGL)	1992	White, R4.2 (US unit R24), 2012
Engineering (EGRb-R6.3) (8.88 m AGL)	1990	Black, R6.3 (US unit R36), 2009

100

101 Figure 1 shows the plan view of the buildings at PPPL and the markings indicate the locations of  
 102 our heat flux plate, thermocouple, and weather station installations (detailed later). LSB is a four-  
 103 story commercial office building. The roof membranes and the insulation foams were newly  
 104 installed in Summer 2012. Apart from the PolyIso foam, a layer of Densdeck was added between  
 105 the membrane and the PolyIso. For the specific purposes of this study, a black EPDM membrane  
 106 was installed over half of the test roof, while the other half was covered with a white EPDM  
 107 membrane. Both parts were manufactured by Carlisle Technology and installed in the same way;  
 108 the sensors were embedded at points with identical R-values (the R-value is typically not  
 109 homogeneous over a roof; it varies horizontally to allow a tapered surface that enhances water  
 110 drainage). The EGR building, mostly utilized for office space, had a roofing structure that also



111 includes plywood insulation between the top membrane and the insulating PolyIso foam. The last  
 112 two sites were on top of the ADM and THY building. Both sites contained no additional layers  
 113 apart from the membrane and the foam. It is important to note (see Table 1) that all the sites  
 114 varied in either their R-values or their albedos. From here on, the roof installations would be  
 115 referred by their respective building names, followed by 'b' or 'w' to indicate the membrane  
 116 color, and then hyphenated by their corresponding R-values.



117  
 118 Figure 1: Map illustrating the buildings and roof installation at PPPL test site. The sensors inside  
 119 the roof layers were placed very close to installed automated weather stations, but at a sufficient  
 120 distance to the south of the stations that ensured the roofs over the sensors were not shaded by  
 121 the weather stations.

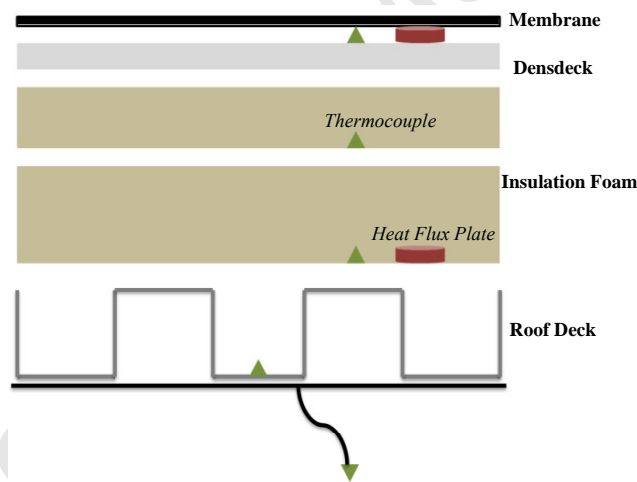
122 All data were logged with Campbell Scientific CR 1000 loggers; measurements were taken at 1

123 Hz but averaged and outputted every one minute. Type-T thermocouples (TC) by OMEGA  
124 Engineering made from “Special Limits of Error Wire” with glass-braded insulation of the  
125 junction were used everywhere. The accuracy, computed following the recommended approach  
126 of the data logger manufacturer and with the parameters provided by TC manufacturer (depends  
127 on many parameters such as the temperature at the reference junction and the measurement  
128 junction) under the experimental condition was estimated to be better than  $\pm 0.1$  K. A subset of  
129 the TCs were also compared in the lab before deployment over a range of temperatures and  
130 showed maximum differences between the sensors of less than 0.2 K (confirming a precision of  
131 also  $\pm 0.1$  K). High-performance heat flux plates from Hukseflux, the PU22 model, which is 3  
132 mm thick and 50 mm in diameter (sensitive area is a  $20 \times 20$  mm square), were used. The  
133 manufacturer specified relative accuracy is  $\pm 5\%$ . The inter-plate comparison conducted in the  
134 lab on a subset of the heat flux plates and suggested differences between the plates that are  
135 smaller than  $\pm 5\%$ . The more relevant finding from these tests is that a standard heat flux plate  
136 that is typically used for soil measurements (Hukseflux model HFP 01) was also evaluated and  
137 showed much larger errors (up to about  $7 \text{ W m}^{-2}$ ). This underlines the importance of using these  
138 high-accuracy thin plates in roof applications where the measured fluxes can be very small and  
139 errors related to plate storage and other factors can become important. This is in agreement with  
140 the recommendations of Meyn and Oke [19], who also found that thin plates are needed for  
141 building applications under some conditions.

142 Five thermocouples and 2 heat flux plates were installed on each roof, except in the ADMw-R8.4  
143 roof where three heat flux plates were used. A roof installation example from the engineering  
144 building is shown in figure 2 and the details of the membrane and insulation layers for all roofs  
145 are provided in Table 2. The depths below the outer surface where the heat flux plates and

146 thermocouples were installed are detailed in table 3. At all sites, a thermocouple was installed  
 147 underneath the membrane, another in the middle of the insulation foam, and a third at the  
 148 interface of building insulation and roof deck; a fourth thermocouple was fixed to the underside  
 149 of the building deck and a fifth was installed in the air plenum. The heat flux plates were  
 150 installed underneath the membrane and between the insulation foam and the roof deck; in the  
 151 admin building (ADM) an additional plate was installed close to the middle of the insulation  
 152 layer. At all sites, the roof deck was either concrete or corrugated steel. The plates and sensors at  
 153 the interface of the insulation and deck were installed at the metal-insulation interface (rather  
 154 than the air-insulation interface).

155



156

157 Figure 2: An illustration of heat flux plate and thermocouple installation at PPPL – from the  
 158 engineering building (the white spaces in between the layers are not air gaps, but are included in  
 159 the figure for clarity of illustration).

160

161

162

Table 2: Roof Installation.

Roof	Membrane	Insulation	Deck
Admin (ADMw-R8.4)	White, 1.5 mm	20.3 cm PolyIso Foam	Concrete
Theory (THYb-R3.7)	Black, 1.5 mm	8.9 cm PolyIso Foam	Corrugated metal
Lyman Spitzer (LSBb-R4.2)	Black, 1.5 mm	1.6 cm Densdeck+ 8.9 cm PolyIso Foam	Corrugated metal
Lyman Spitzer (LSBw-R4.2)	White, 3.7 mm	1.6 cm Densdeck+ 8.9 cm PolyIso Foam	Corrugated metal
Engineering (EGRb-R6.3)	Black, 2.3 mm	1.3 cm Wood+ 13.4 cm PolyIso Foam	Corrugated metal

163

164

165 Table 3: Thermocouple and Heat Flux plate installation depths. The table lists the depths of the  
 166 upper 3 thermocouples (\* 4 for EGRb). The lowest two thermocouples were installed at the lower  
 167 surface of the roof deck (pasted to the surface) and in the underlying air plenum. At EGR no  
 168 thermocouple was installed on the lower roof deck surface.

Roof	Thermocouple Installation Depths (cm from roof surface)	Heat Flux Plates Installation Depths (cm from roof surface)
ADMw-R8.4	0.2, 10.3, 20.5	0.2, 10.3, 20.5
THYb-R3.7	0.2, 4.6, 9.0	0.2, 9.0
LSBb-R4.2	0.2, 5.6, 10.7	0.2, 10.7
LSBw-R4.2	0.4, 5.8, 10.9	0.4, 10.9
EGRb-R6.3	0.2, 1.5, 5.3, 14.8*	0.2, 14.8

169 Apart from the thermocouple and the heat flux plates, the ambient weather conditions were  
170 monitored using wireless Sensorscope® stations (<http://www.sensorscope.ch/> [20], see details of  
171 all sensors specifically deployed on the stations used here in [21]). These mobile meteorological  
172 towers, each 2 m tall, were placed next to the roof installations at all the sites but were not  
173 shading the roof over the embedded sensors. In addition to the ambient weather conditions, these  
174 instruments monitored surface temperature and albedo.

175 While combinations of thermocouples and heat flux plates have been previously used to estimate  
176 the storage flux in urban areas including roofs before [8], [19], and also to test different roofing  
177 elements under laboratory conditions [9]-[11], [22], [23], our study is unique in the extensive  
178 monitoring of 5 roofs that vary both in insulation and albedo at a single site (same  
179 meteorological conditions). The comparison of LSB white and black roofs, which are exactly  
180 identical in age, construction, and design, is also a critical feature of this study.

181  
182 The experimental data collection started in late July of 2012 and is ongoing; here we use data  
183 from August 2012 to July 2013. It should be noted that there weren't any extended periods when  
184 the incident weather was abnormal. The heat flux plates sampled data at 1-minute resolution and  
185 were checked for erroneous data points and spikes.

186

### 187 **3 Results**

188 The collected data were analyzed to understand the effect of insulation R-value and roof  
189 albedo on heat fluxes into the deck. As noted before, 4 of the decks consisted of corrugated  
190 metal that offered no further resistance to heat flux and hence fluxes at the bottom of the  
191 insulation layer are essentially the fluxes into the indoor space. The administration

192 building (ADMw-R8.4) had a concrete deck. But to be able to compare the 5 sites in a  
193 consistent manner, we will ignore the additional resistance this concrete deck offers and  
194 simply compare fluxes at the bottom of the insulation layers. It should however be noted  
195 that this concrete deck will have a significant influence on the heat entering the building. A  
196 focus of our study is also to understand how the albedo and R-value effects interact. To  
197 illustrate such interaction with a simple example, one can consider a very highly insulated  
198 roof, say R-40; it is obvious that the albedo of such a roof has no impact on building energy  
199 consumption since almost no heat flux will reach the bottom of the insulation. In more  
200 practical cases, with an R-value less than 9, the effect of the albedo will increase as the R  
201 decreases and the theoretical maximum albedo effect occurs when  $R = 0$ .

202

### 203 **3.1 Summer Temperature and Heat Flux Profiles**

204 Figure 3 depicts profiles of temperature inside the five roof structures for various times of the  
205 day, where each profile is the average of all the individual profiles occurring at that time during  
206 August 2012. That is, the figure describes the evolution of temperature over an average August  
207 day inside various roof structures. The timestamps shown in figure 3 are in EDT (UTC-0400).  
208 The zero level in the profiles refers to the top of the roof, just underneath the membrane and the  
209 depth then increases, as we get closer to the building's roof deck. The topmost value represents  
210 the temperature directly underneath the roof's EPDM membrane and the bottom measurement  
211 denotes the temperature at the interface of insulation foam and roof deck. The measurements  
212 inside the building are omitted since they are not affected by the time of day in the same way as  
213 external temperatures (due to air conditioning) are and would confuse the reader. In general these  
214 two internal temperatures were similar and did not fluctuate much during a typical day.

215 During the night and early morning hours (0015 and 0415), the temperature underneath the  
216 membrane is around 13-15 °C and it keeps increasing, as we get closer to the roof deck; these  
217 low temperatures are the result of cooling of the surface by longwave radiation emission and are  
218 lower than external air temperatures, which averaged around 19 °C in August 2012. During this  
219 period, the temperature at the air plenum for all the rooftops was around 23-25 °C on average.  
220 The structure of the temperature profiles during these late night and early morning hours thus  
221 clearly indicates a negative heat transfer, i.e., energy lost from the buildings to the surroundings.  
222 This allows the buildings to cool down at night. An important feature to underline is that, during  
223 nighttime, the outer surface temperatures are the same over the white and black roofs. This is  
224 expected since albedo plays no role at night, and the emissivities of the two roofs are about  
225 equal.

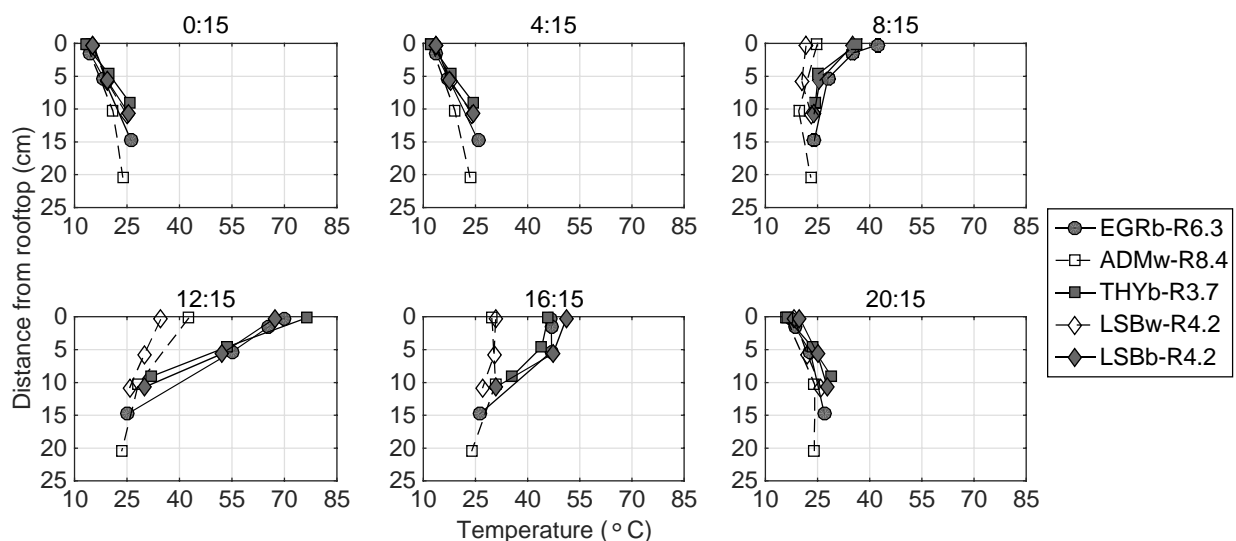
226 However, around 0815 local time, as incoming solar radiation starts increasing, the black roofs  
227 transition and start absorbing significant amounts of thermal energy. In contrast, the highly  
228 reflective ADMw-R8.4 and LSBw-R4.2 roofs are slower to react. One interesting phenomenon  
229 to note during this time period (0815) occurs over the ADMw-R8.4; the insulation element or  
230 temperature sensor at the third depth is at a lower temperature compared to the roof deck below  
231 it and the membrane above it. This minimum is expected to occur since the heat flux at the upper  
232 surface starts inverting the temperature profiles inside the roof leading to a point where the slope  
233 changes sign. At the ADMw-R8.4, which is the most insulated, the difference between depth 1  
234 and 2 and depth 2 and 3 is around 5 °C.

235 During the midday period, the temperature profiles are completely reversed; the membrane  
236 temperature is higher than that of the roof deck. The black roofs are about 30 °C warmer than the  
237 white roofs at the outer surface: all three black roofs have membrane temperatures around 65-75

238 °C, whereas the white roofs ADMw-R8.4 and LSBw-R4.2 have temperatures of 42 °C and 35 °C  
 239 respectively. A second transition occurs during the evening period, around 1615 local time, when  
 240 the roofs begin to cool. Their surface temperatures being very elevated, they now radiate,  
 241 convect, and reflect more energy than they receive despite the fact that shortwave solar radiation  
 242 is still quite significant at that time. As expected, the black roofs cool faster between 1215 and  
 243 1615: the black roof membrane temperatures drop by almost 30 °C compared to a 10 °C  
 244 observed drop for the white membranes.

245 At night, around 2015 local time, the temperature profiles are reversed again. The membranes  
 246 become cooler than the roof decks as the surface continues to lose heat to the surrounding  
 247 environment by radiation. During this time period though, the temperature at depth 3 was higher  
 248 than the temperature at the deck and plenum (not shown here) for all the sites indicating that  
 249 outward heat flux from the building, which was observed at 0015 starts later at night.

250



251

252 Figure 3: Monthly-averaged temperature profiles at specific times over various roof structures  
 253 for August 2012, time is EDT (note that black roof markers are filled in gray and white roof  
 254 markers are unfilled/white).



255 The profiles of temperature inside the roof structures clearly illustrate the periodicity of the  
256 thermal dynamics at play during the warmer month. All five roof structures, irrespective of their  
257 albedo and insulation thickness, transition from a heat source for the indoor space during the day  
258 to a heat sink for the indoor space at night. However, the magnitude of the shift and the heat  
259 sources and sinks the indoor space experiences clearly depend on the albedo and the insulation  
260 thickness of the roof structures. The insulation was also found to cause a phase shift (delay) in  
261 heat transfer due to its thermal inertia, leading to maxima and minima in the temperature profiles  
262 occurring inside the roof layers at various times; thicker insulation naturally produced larger  
263 shifts.

264 This section will focus on how the temperature profiles discussed in the last section translated to  
265 heat fluxes, but unlike the five levels of temperature measurements, the heat flux plates were  
266 only installed at two levels due mainly to their high cost. Recall that these two levels are at the  
267 top of the roof, underneath the membrane, and at the bottom, at the interface between roof  
268 insulation and the solid deck. ADMw-R8.4 had one extra heat flux plate towards the middle.

269 Figure 4 shows averaged profiles of heat flux inside five roof structures (same y-axis scale as  
270 Figure 3). These are also the averaged fluxes, at those times, over all the days of August 2012.

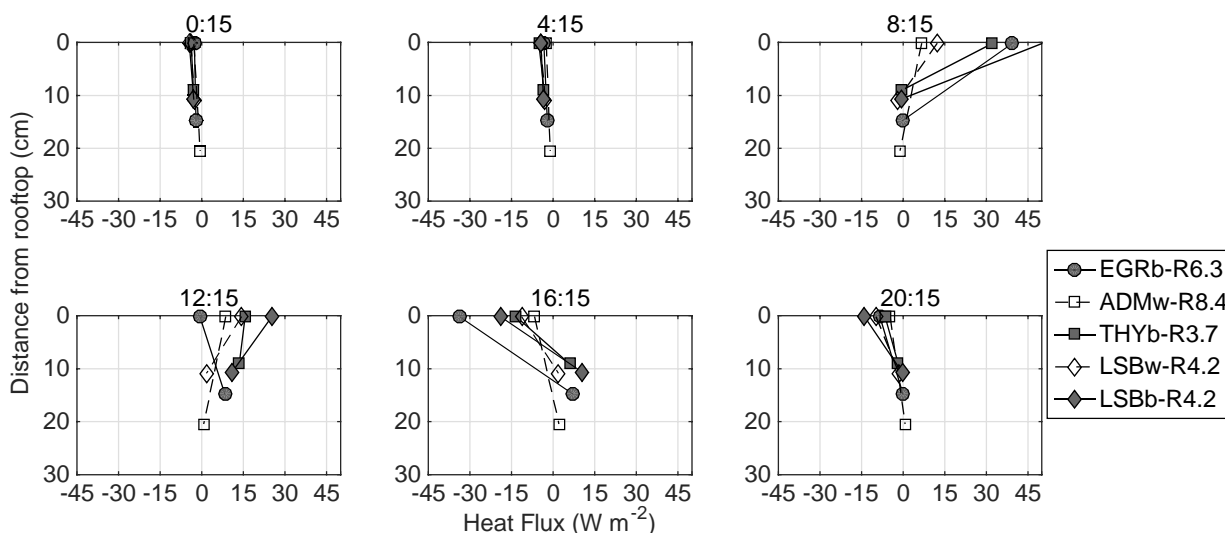
271 As expected from the temperature profiles, at night, there is a net negative heat flux indicating  
272 loss of energy from the buildings; however, it is important to note that more energy is lost from  
273 the top membrane layer compared to the bottom. The differences between top and bottom fluxes  
274 are  $0.6\text{-}1.3 \text{ Wm}^{-2}$ , with the more insulated roof structures losing less heat at the bottom  
275 compared to the relatively thin insulated structures. However, the fluxes versus depth profiles  
276 collapse suggesting that the lower bottom losses in the thicker roofs are directly attributable to  
277 the higher thermal inertia of these roofs (surface cooling takes longer to be felt at larger depths).

278 At 0415, while the structure of the heat flux profile remains identical to that of 0015, the  
279 magnitude of heat loss increases slightly despite the fact that surface temperature are not  
280 significantly different; this increase in surface cooling might be related to the atmospheric  
281 cooling and the concomitant reduction in downwelling longwave radiation. During the morning  
282 transition period, while the bottom heat flux remains slightly negative ( $\sim -1.5 \text{ Wm}^{-2}$ ) at all sites,  
283 the exterior surfaces actively absorb incoming solar radiation producing a downward (positive)  
284 heat flux at the top. At EGRb-R6.3 for example, while the heat flux at the bottom is  $-0.6 \text{ Wm}^{-2}$ ,  
285 the membrane absorbs nearly  $40 \text{ Wm}^{-2}$ . The temperature of all surface rise considerable as  
286 illustrated previously in figure 3.

287 As the surface temperatures rise, the roofs start losing larger heat fluxes by radiative and  
288 convective transfer to the atmosphere. Therefore, by 1215 local time, the net heat fluxes at the  
289 top decrease considerably, and for EGRb-R6.3 they even switch to net heat losses at the top; all  
290 other roof structures continue to actively absorb heat but at lower magnitudes than in the early  
291 morning. This quick transition observed at EGRb-R6.3 is related to the low thermal capacity of  
292 the plywood underlying the membrane, which is used as a secondary insulation layer separating  
293 the membrane from the PolyIso foam. The low heat capacity implies lower thermal inertia,  
294 which results in rapid responses of EGRb-R6.3: it heats fast (highest surface temperature at  
295 0815) and then switches regime the earliest. Over all roof structures, the fluxes at the bottom are  
296 positive (into the building) at 1215, but the black roofs clearly conduct higher fluxes into the  
297 indoor space.

298 At 1615, the top of the insulation layer cools down and releases heat into the atmosphere over all  
299 roofs; however, the bottom parts are still conducting the heat stored inside the roof layers into the  
300 buildings. By nighttime (2015), while the bottom layers cool down substantially (bottom heat

301 fluxes close to 0, recall from the temperature profiles that small negative fluxes develop later  
 302 during the night), the top membranes actively lose heat at up to  $-15 \text{ W m}^{-2}$ .  
 303

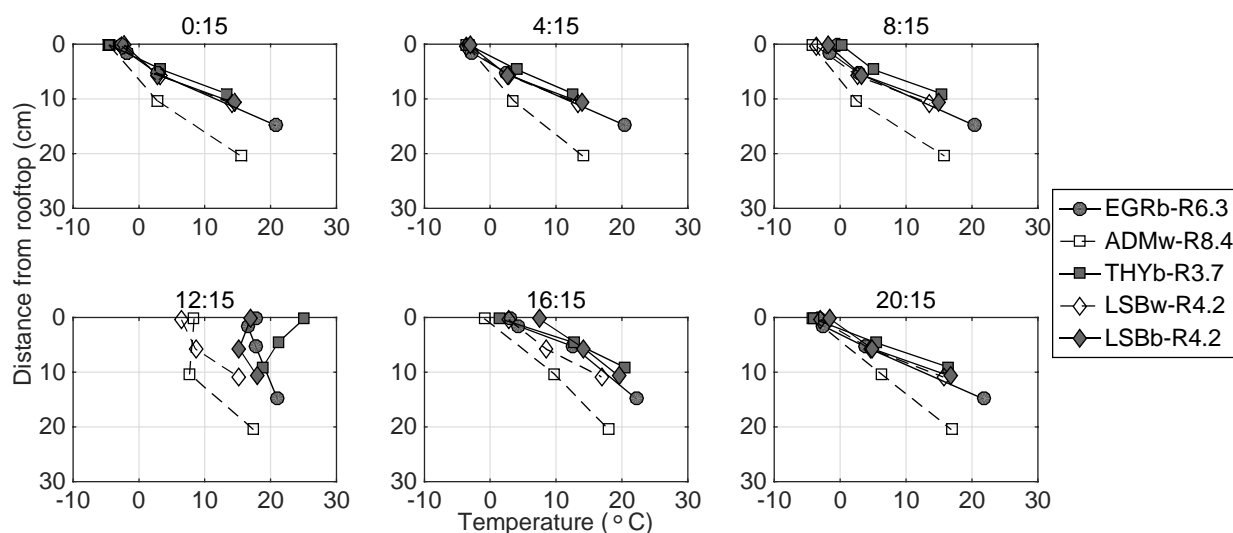


304  
 305 Figure 4: Averaged heat flux profiles over different roof structures for August 2012; times in  
 306 EDT (note that black roof markers are filled in gray and white roof markers are unfilled/white).

307  
 308 **3.2 Winter Temperature and Heat Flux Profiles**

309 The previous sections analyzed temperature and heat flux profiles for August 2012, a summer  
 310 month; this section will compare those observations to January 2013, the coldest month of the  
 311 observational period. The average air temperature in January was  $1.3^\circ\text{C}$  compared to  $23.8^\circ\text{C}$  in  
 312 August. The timestamps above the plots are here in EST (UTC-0500). Figures 5 and 6 show  
 313 monthly-averaged profiles of temperature and heat flux, calculated in identical fashion to the  
 314 summer months. From the figures, it is clear that the top membrane temperature for all the  
 315 rooftops averages around  $5^\circ\text{C}$  at 0015, 0415, 0815 and 2015 hrs, in fact they only change during  
 316 the midday and afternoon periods (1215 and 1615 hrs) due to the reduced length of insolation in  
 317 the winter in Princeton, NJ. During all time periods, there exists a negative gradient between

318 depths 2 and 3, indicating heat transfer from the building into the insulation layers, except at  
 319 THYb-R3.7 during the midday period. For THYb-R3.7, the profile is inverted at 1215, indicating  
 320 a downward heat flux in the lower parts of the insulation layer that can be directly attributed to  
 321 its low insulation thickness allowing the downward heat flux front to reach the bottom within the  
 322 period where solar radiation is heating the external membrane. However, this downward heat  
 323 flux in the THYb-R3.7 insulation layer is not translated into heat gains for the indoor space:  
 324 unlike the warmer month, a transition of the roof from being a sink of heat to being a source  
 325 never really materializes in the winter months and the buildings are continuously losing energy  
 326 to the surrounding. This can be concluded by noting that the plenum temperatures (lowest level)  
 327 remain around 15-22 °C for the buildings, which is higher than the bottom insulation temperature  
 328 even for THYb-R3.7 at 1215.



329

330 Figure 5: Averaged temperature profiles over different roofs for January 2013

331

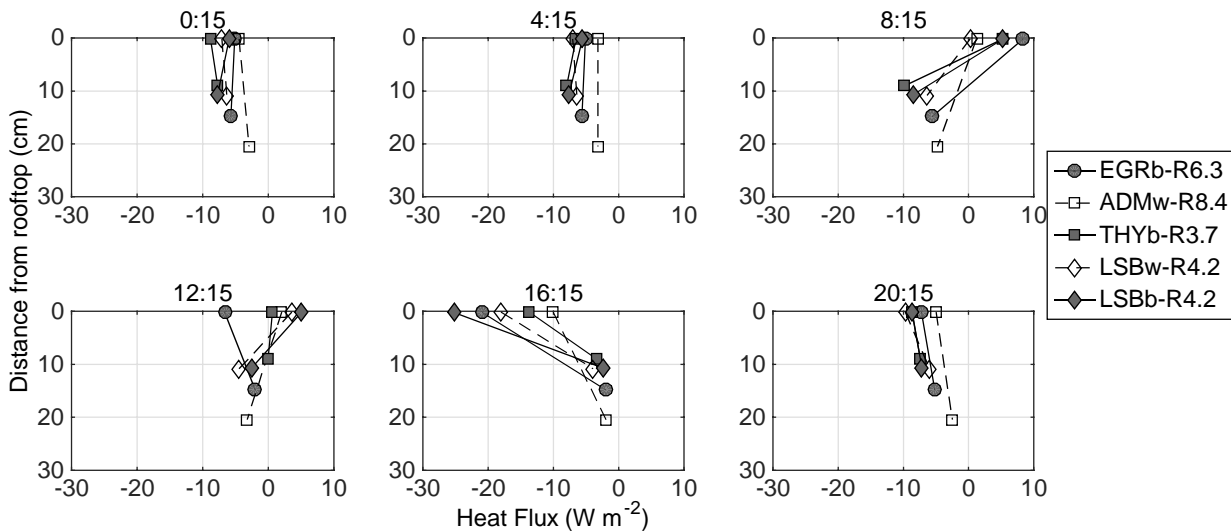
332 Figure 6 shows the heat flux profiles for January 2013. The midnight and early morning heat flux  
 333 profiles from January suggest flux homogeneity over the entire roofing depth and the

334 surrounding environment (except for LSBb-R4.2 where the fluxes still vary with depth, albeit  
335 mildly). The lack of significant flux gradient indicates that the heat lost at both the top and  
336 bottom of the roof is roughly the same for all the structures. This is attributed to the length of the  
337 nighttime condition during the winter that allow temperature profiles in the insulation layer to  
338 become linear, as revealed in Figure 5. The influence of insulation is visible in all the subplots:  
339 the ADMw-R8.4 consistently experiences the lowest heat transfer compared to all other roof  
340 structures at almost all time periods. At midnight, while all other roofs loose around  $-4 \text{ Wm}^{-2}$  at  
341 the bottom, the heat lost at ADMw-R8.4 roof is half that amount.

342 It is important to note that the highest energy losses from the top membrane, rather than  
343 occurring in the middle of the night, occur in the afternoon around 1615 when the top most layer  
344 is loosing on average around  $-10 \text{ Wm}^{-2}$  at THYb-R3.7, LSBw-R4.2 and EGRb-R6.3, while the  
345 LSBb-R4.2 roof is loosing around  $-15 \text{ Wm}^{-2}$ . This sudden increase in upward heat flux at 1615  
346 occurs also in August. Both the summer and winter peaks in upward fluxes at 1615 are due to the  
347 decrease in solar radiation coinciding with the peak in surface temperatures that the roofs reach  
348 at those times. These factors combine to maximize longwave radiative and convective cooling  
349 and to reduce solar radiative gain such that the energy budget of the roof becomes in deficit, and  
350 upward flux from the insulation layer is maximized to balance the budget and sustain the surface  
351 cooling. But these fluxes do not necessarily translate into upward fluxes at the bottom of the  
352 insulation due to the thermal inertia of the layer.

353 As suggested by the temperature profiles, the fluxes at the bottom of the insulation are always  
354 negative, and hence the roof structures acts as a heat sink for the indoor space at all time periods,  
355 absorbing thermal energy. The top part of the roof, while mostly loosing heat to the exterior,  
356 switches to gaining heat during the early morning to midday period where it receives high

357 shortwave solar radiative flux, particularly for black roofs. However, this gain is short-lived and  
 358 all roofs revert to losing heat at 1615, when strong longwave radiative cooling occurs. The  
 359 black roofs, THYb-R3.7 and LSBb-R4.2 absorb the most during the mid-day period, 6 and 12  
 360  $\text{Wm}^{-2}$  respectively, due to their high peak temperatures.



361  
 362 Figure 6: Averaged heat flux profiles over different roof structures for January 2013.

363 Comparing the August and January profiles one can note that for the peak cooling loads (peak  
 364 summertime positive fluxes at the bottom of insulation at 1215 and 1415), the roofs can be  
 365 clearly segregated based on roof color. For peak heating loads (peak wintertime negative fluxes  
 366 at the bottom of insulation at 0015 and 0415), the fluxes seem to vary almost linearly with  
 367 insulation depth and roof color plays a minor role. This is expected since roof color has no  
 368 bearing on the thermal dynamics when there is no solar radiation at night, while it is very  
 369 important during the solar downwelling radiation daytime peak. These observations are not  
 370 entirely surprising, but they will be very important later in the discussion so we underlined them  
 371 here.

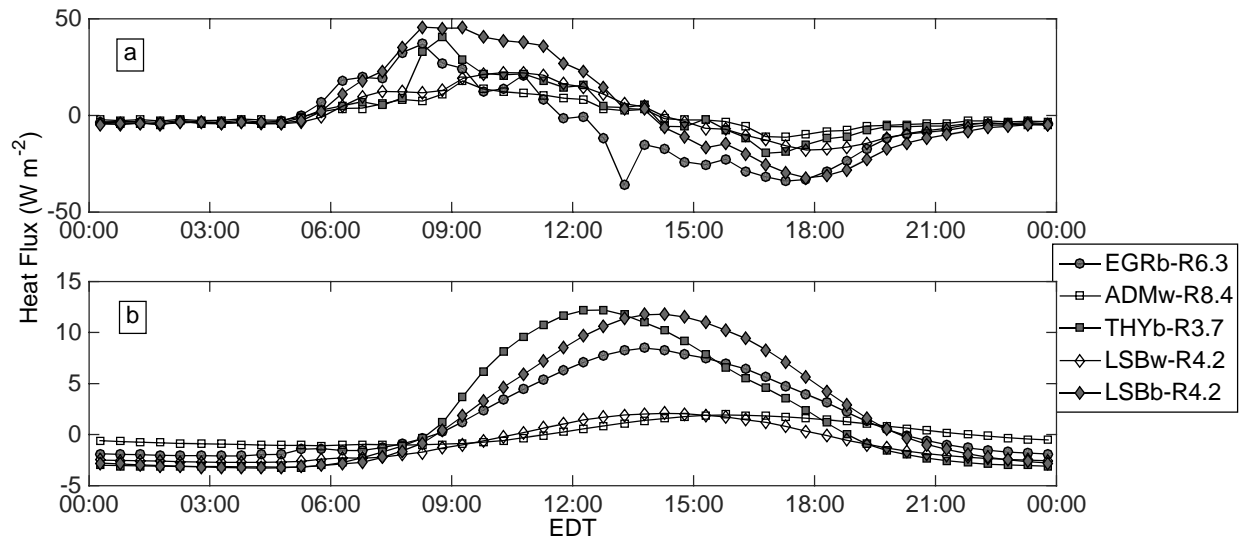
372

### 373 3.3 Diurnal Variation

374 To further understand the daily variation of heat flux over various rooftops, the diurnal cycles of  
375 30-minute-averaged heat fluxes from the top and bottom plates were averaged for different  
376 months. Figure 7 shows this variation for all roof structures for August 2012. The average daily  
377 maximum air temperature during this month was around 30°C and the average lows were close  
378 to 21°C. The total precipitation was 25 mm. It is obvious from the graph that there exists a  
379 difference in amplitude and phase between the heat flux directly under the membrane and the  
380 flux at the bottom of the insulation. The black roofs EGRb-R6.3, LSBb-R4.2 and THYb-R3.7 all  
381 have peaks around 40-50  $\text{Wm}^{-2}$ . In stark contrast the white roofs LSBw-R4.2 and ADMw-R8.4  
382 peak at 15-20  $\text{Wm}^{-2}$ . This dissimilarity observed in the magnitude of heat fluxes is directly  
383 related to the difference in albedos. In addition the higher albedo over white roofs is also  
384 responsible for maintaining the heat flux values close to zero when the incoming solar radiation  
385 is low. Over the black roofs during the late afternoon hours, while the atmosphere is rapidly  
386 cooling, high negative fluxes are observed. Albedo is also responsible for the reduced heat fluxes  
387 at the bottom of the roof. While the peak heat flux at the bottom over white roofs average  
388 around 2-4  $\text{Wm}^{-2}$  the heat flux recorded at the bottom of black roofs peak around 12-14  $\text{Wm}^{-2}$ .  
389 But it is interesting to note that even among the heat fluxes observed at the top, the black roofs  
390 peak much earlier compared to white ones. The black roofs, at the top, have flux peaks around  
391 0800 EDT, whereas the white roofs peaks around 0930-1000 EDT. As described above, the  
392 black roofs peak around 40-50  $\text{Wm}^{-2}$  and the white roofs peak at much lower value, 15-20  $\text{Wm}^{-2}$ .  
393 This difference in magnitude and phase is directly related to the effect of the roof albedos.  
394 Apart from differences in albedo, insulation thickness and ageing of the membrane also  
395 contribute to the dissimilarities observed.

396 The diurnal variations in temperature and heat flux profiles indicate the complex role played by  
 397 the roof's thermal inertia. While it is evident that the membrane albedo restricts the heat  
 398 exchanged between the roof and the surrounding environment, insulation thickness plays a  
 399 crucial role in delaying the transfer of this heat indoors. Figures 7a and b show that, while the  
 400 heat fluxes below the membrane peak around 0800-1000 local time, the bottom peaks are  
 401 delayed by at least 2 hours and vary with insulation thickness. The THYb-R3.7 roof peaks  
 402 around midday, while the other roofs peak during the early afternoon periods. Peak times are  
 403 quite important since the phase shifts in heat gains over well insulated roofs could be used  
 404 effectively to spread out the cooling loads more evenly in time by delaying the flux from the roof  
 405 compared to the flux from windows and from air exchanges (these have the same phase as air  
 406 temperature, which peaks in the early afternoon).

407



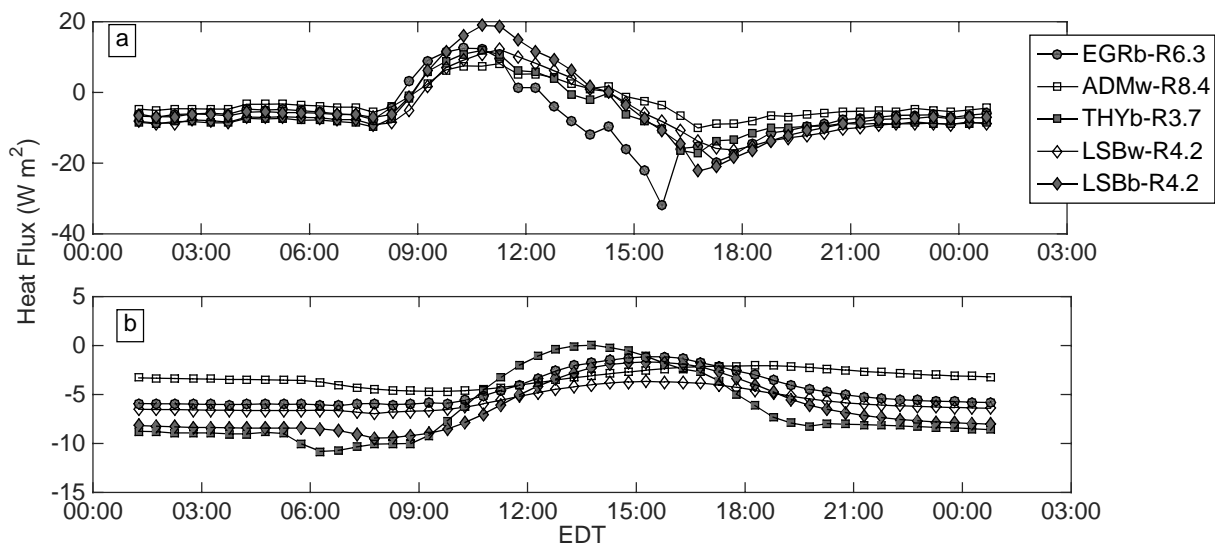
408

409 Figure 7: Averaged diurnal variation of heat flux at the top (top panel) and bottom (bottom  
 410 panel) of different roof structures for August 2012.

411



412 Figure 8 describes the monthly averaged diurnal variation of top and bottom heat fluxes for  
 413 January 2013. During January 2013 the ambient air temperature peaks averaged around 2 °C and  
 414 the lows averaged around -2.5 °C. As expected during January (Figure 8), the maximum heat  
 415 flux values at the top are much lower than during the summer. LSBb peaks are about 18 Wm<sup>-2</sup>;  
 416 EGRb-R8.4 and THYb-R3.7, the other black roofs, both have peaks around 12 Wm<sup>-2</sup>. The phase  
 417 difference between top and bottom fluxes is clearly visible and depends on insulation thickness,  
 418 but not on albedo since the LSBw-R4.2 and LSBb-R4.2 roofs fluxes peak at the same time  
 419 (around 1100 at the top and 1530 at the bottom). At the bottom, figure 8b, the THYb-R3.7 roof,  
 420 which has the lowest insulation is the only roof structure that exhibits very small positive fluxes  
 421 during peak insolation time. All other roofs fluxes remain negative, i.e. they continue to cause  
 422 heat loss from the buildings all day long. As expected, the ADMw-R8.4, which has the highest  
 423 insulation, allows the least amount of fluxes out and its diurnal cycle remains quite flat,  
 424 indicating less variability relative to other roof structures.



425

426 Figure 8: Averaged diurnal variation of heat flux at top and bottom of different roof  
 427 structures for January 2013.

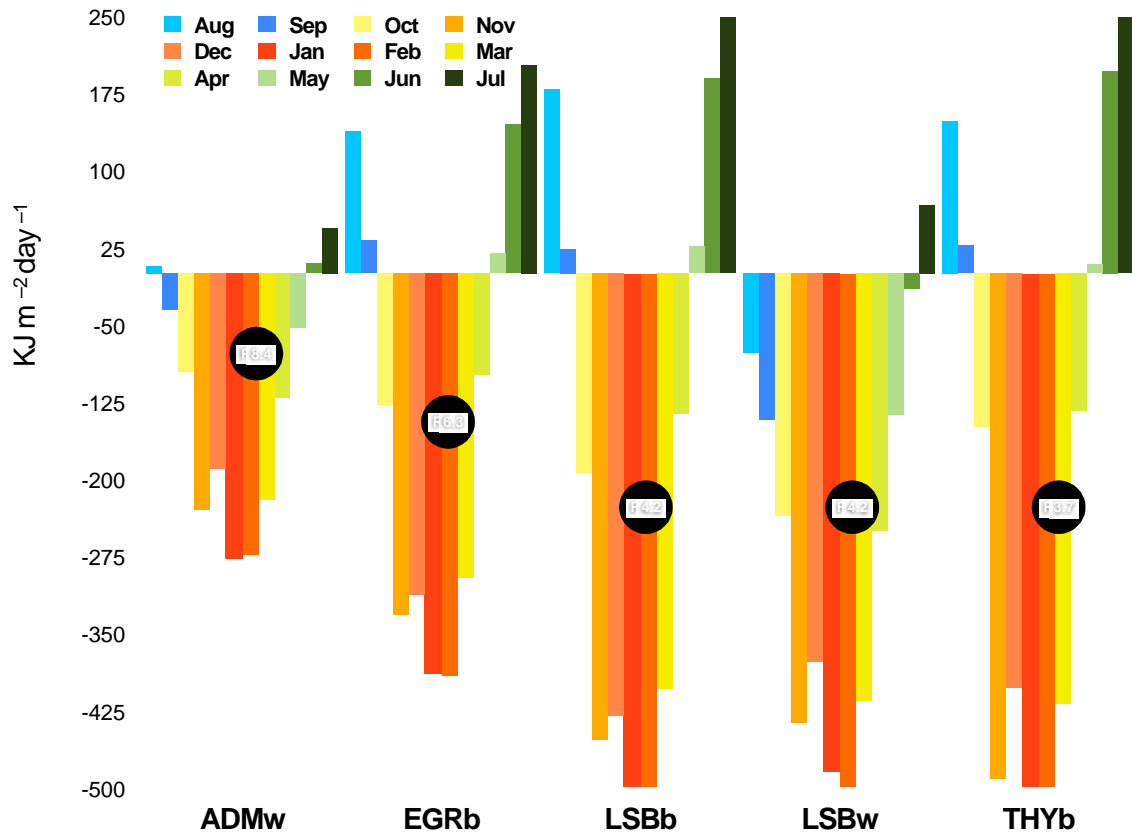
428

### 429 3.4 Average Heat Flux

430 Figure 9 shows the average energy in  $\text{KJ m}^{-2} \text{day}^{-1}$  that enters (positive) or leaves (negative) the  
431 building (bottom of insulation). Data from the bottom-most heat flux plate were integrated over  
432 each day and averaged over a whole month to obtain the monthly bar chart of daily heat fluxes.  
433 The chart shows that, during the warmer months, August, September, May, June and July the  
434 black roofs act as a net source of energy for the indoor space, whereas the white roofs, especially  
435 LSBw-R4.2, acts as a net sink. LSBw-R4.2 releases 76, 140, 136 and 14  $\text{KJ m}^{-2} \text{day}^{-1}$  for  
436 August, September, May and June, while ADMw-R8.4 has small net gain during August, June  
437 and July (7.6, 10 and 45  $\text{KJ m}^{-2} \text{day}^{-1}$  respectively), but acts as a sink in September and May (34  
438 and 53  $\text{KJ m}^{-2} \text{day}^{-1}$  respectively). This is very much due to the albedo of the membrane. The  
439 LSBw-R4.2 roof was newly laid in Summer 2012 and has an albedo close to 0.55 compared to  
440 the older membrane on ADMw-R8.4, which has an albedo around 0.35.

441 During the colder months, the insulation thickness plays a much more dominant role than albedo.  
442 A direct correlation can be seen between the energy lost from the buildings and their R-values.  
443 The ADMw-R8.4, loses the least amount of energy. In November, the ADMw-R8.4 suffers a  
444 net loss of 230  $\text{KJ m}^{-2} \text{day}^{-1}$  whereas the THYb-R3.7 loses 490  $\text{KJ m}^{-2} \text{day}^{-1}$ . The LSBw-R4.2  
445 and LSBb-R4.2, the identical new roof structures, lose around 436 and 450  $\text{KJ m}^{-2} \text{day}^{-1}$ ,  
446 respectively. The EGRb-R6.3 loses close to 330  $\text{KJ m}^{-2} \text{day}^{-1}$ . The bars indicate that doubling  
447 the insulation almost halves the losses; this is consistent with the fact that the heat flux in the  
448 roof  $Q$ , under steady state conditions, should scale as  $Q \sim 1/R$ . The plots also show that, as the  
449 membrane ages, it loses its effectiveness. The LSBw-R4.2 roof, which is very new, has almost  
450 twice the albedo of the ADMw-R8.4 roof.

451 One surprising finding was that during December, less heat was lost compared to November. A  
452 closer inspection of the difference between the indoor temperatures measured at the air plenum  
453 and the temperature at the bottom of the insulation foam revealed a higher difference (about  
454 0.5 °C higher) during November compared to December. Given that December was colder  
455 (leading to higher temperatures at the bottom of the insulation), this indicates that indoor  
456 temperatures remained higher in November. This could either be due to the pronounced  
457 entrainment of colder outside air through hallways, doors and windows during December thereby  
458 considerably reducing the indoor temperature or due to reduced indoor heating during the Winter  
459 break at the end of December.



460

461 Figure 9: Averaged daily heat flux in/out of roof structures from August 2012 – July 2013. A  
 462 positive value indicates heat absorbed by the building while a negative flux indicates heat lost by  
 463 the building.

464 Finally, it should be noted that aging and temperature do affect the heat flux measured,  
 465 however it is impossible to attribute the individual contribution of these effects as it  
 466 requires continuous observation of changes in physical properties (thermal conductivity  
 467 and thermal capacity of the insulation foam and roof membrane) of the roof material.  
 468 Nevertheless, while aging and temperature effects reduce the thermal efficiency of the roof  
 469 structure in moderating the heat entering and leaving the building envelope, the large scale  
 470 differences noticed here are primarily a factor of insulation thickness and membrane  
 471 reflectivity. As one can infer from Figure 9, the LSBw-R4.2 and LSBb-R4.2 roofs which have

472 identical roof insulation and were laid at the same time (Summer 2012), let in the same  
473 amount of heat during the winter months (around  $-450$  to  $-500$   $\text{KJ m}^{-2} \text{ day}^{-1}$  for January and  
474 February) when the effect of insulation thickness is pronounced, but during the summer  
475 months have significantly different values, around  $250$   $\text{KJ m}^{-2} \text{ day}^{-1}$  for LSBb-R4.2 and  $\text{KJ m}^{-2}$   
476  $\text{ day}^{-1}$  for LSBw-R4.2 in July. Furthermore, the ADM and EGR roofs which are older  
477 compared to LSBw-R4.2 and LSBb-R4.2 roofs but have higher insulation thickness, let out  
478 less heat during the winter months. The ADMw-R8.4 which has an R value of 8.4 let out -  
479  $275$   $\text{KJ m}^{-2} \text{ day}^{-1}$  of heat in December compared to  $-500$   $\text{KJ m}^{-2} \text{ day}^{-1}$  let out by the newly  
480 laid LSBw-R4.2 and LSBb-R4.2, both of which have an R value of 4.2. These results indicate  
481 that any effects of aging and temperature will only strengthen our argument, as it will  
482 widen the difference between the less insulated and more insulated roofs. Finally, while the  
483 experimental set up did not account for aging and temperature effects independently, the  
484 wide range of insulation and albedo values of the roof structures studied in the experiment  
485 unequivocally proves insulation thickness and albedo as the primary factors in determining  
486 the energy entering or leaving the roof top.

487

#### 488 **4 Summary and Conclusions**

489 Detailed experimental measurements inside five roofs with different albedos and insulation R-  
490 values were conducted to understand the interacting roles of these two roof characteristics on the  
491 building energy performance. The results reveal the complex transient dynamics of heat transfer  
492 through heterogeneous roof structures. Apart from the relatively well-understood effects of  
493 membrane albedo, the thermal storage capacity of the roof elements also plays a significant role

494 in controlling the transfer of energy through roof structures, and this role is also affected by the  
495 roof albedo.

496 Our results indicate that white membranes are highly effective in reducing the cooling load  
497 during the warmer months; insulation thickness (R-values) on the other hand controls the heating  
498 loads during winter periods. The observations indicate that doubling the R-value leads to halving  
499 the amount of heat transferred, irrespective of the membrane albedo; this is consistent with the  
500 fact that heat loss under steady state conditions scale as  $1/R$ . But at what level this becomes  
501 financially ineffective needs to be explored more thoroughly.

502 Overall, energy offsets related to reduced heating loads by black roofs during winter periods  
503 were negligible compared to the cooling load reductions allowed by cool roofs during the  
504 summer period, in agreement with previous comparable studies in the region [12]. As indicated  
505 above, insulation thickness played a much more direct role in reducing the heating loads during  
506 the wintertime. The insulation thickness also modulated the phase of heat transfer in the roof,  
507 delaying the fluxes at larger depths compared to fluxes at the top of the roof.

508 Finally, summarizing our findings leads us to conclude that white/reflective membranes with  
509 high R-value should be recommended for the Northeastern US region where our study took  
510 place. The insignificant differences observed between the heating loads of white/cool and black  
511 roofs during winter months, which we linked here to the negligible impact of albedo during peak  
512 heating periods (as opposed to its crucial role during peak cooling), support a broader conclusion  
513 that cool roofs can help reduce building energy consumption in many cold climate areas that  
514 have much higher heating degree days than cooling degree days, which is the case for our study  
515 area (heating degree days are almost 5 times the cooling degree days in Princeton, NJ). The  
516 white membranes, apart from reducing the cooling load in summer months, will also be

517 beneficial in reducing ambient urban temperatures in dense urban neighborhoods and could be a  
518 potential mitigation strategy in reducing the effects of urban heat islands and urban heat stress.  
519 This is particularly important given the potential for synergistic interactions between urban heat  
520 islands and heat waves, the later being expected to exacerbate due to global warming, which can  
521 pose significant health hazards for urban residents [24].

522 While this article dealt exclusively with the observations made at our field site, in the next part of  
523 this study, the results from this analysis will be used to validate a vertically-resolved roof model,  
524 PROM (Princeton Roof Model). The model will then be applied to explore a broader mix of R-  
525 values and albedos and to address some of the unanswered questions from this study, including  
526 at what R-value does the energy transfer plateau? Furthermore, a detailed cost-benefit analysis  
527 will be carried out in parallel to energy savings.

528

### 529 **Acknowledgements**

530 This work was supported by the US Department of Energy through Pennsylvania State  
531 University's Energy Efficiency Building Hub under grant No. DE-EE0004261 and by the Helen  
532 Shipley Hunt Fund through Princeton University. The authors also extend their gratitude to the  
533 staff members at PPPL for their invaluable help in setting up the experiment.

534

### 535 **References:**

- 536 [1] U. D. O. Energy, "2011 Building energy Data Book," 01-Mar-2012. [Online]. Available:  
537 [http://buildingsdatabook.eren.doe.gov/docs/DataBooks/2011\\_BEDB.pdf](http://buildingsdatabook.eren.doe.gov/docs/DataBooks/2011_BEDB.pdf).  
538
- 539 [2] S. J. Konopacki and H. Akbari, "Measured energy savings and demand reduction from a  
540 reflective roof membrane on a large retail store in Austin," Lawrence Berkeley National  
541 Laboratory, LBNL-47149, 2001.  
542
- 543 [3] H. Akbari and R. Levinson, "Evolution of Cool-Roof Standards in the US," *Advances in*

- 544 *Building Energy Research*, vol. 2, no. 1, pp. 1–32, 2008.  
 545  
 546 [4] M. Santamouris, “Cooling the cities—a review of reflective and green roof mitigation  
 547 technologies to fight heat island and improve comfort in urban environments,” *Solar*  
 548 *Energy*, vol. 103, pp. 682–703, 2014.  
 549  
 550 [5] T. Xu, J. Sathaye, H. Akbari, V. Garg, and S. Tetali, “Quantifying the direct benefits of  
 551 cool roofs in an urban setting: Reduced cooling energy use and lowered greenhouse gas  
 552 emissions,” *Building and Environment*, vol. 48, pp. 1–6, Feb. 2012.  
 553  
 554 [6] E. Orbendorfer, J. Lundholm, B. Bass, R. Coffman, H. Doshi, N. Dunnett, S. Gaffin, M.  
 555 Köhler, K. Liu, and B. Rowe, “Green Roofs as Urban Ecosystems: Ecological  
 556 Structures, Functions, and Services,” *BioScience*, vol. 57, no. 10, p. 823, 2007.  
 557  
 558 [7] H. Akbari, M. Pomerantz, and H. Taha, “Cool surfaces and shade trees to reduce energy  
 559 use and improve air quality in urban areas,” *Solar Energy*, vol. 70, no. 3, pp. 295–310,  
 560 Jan. 2001.  
 561  
 562 [8] D. J. Sailor, “A green roof model for building energy simulation programs,” *Energy and*  
 563 *Buildings*, vol. 40, no. 8, pp. 1466–1478, Jan. 2008.  
 564  
 565 [9] A. Pasupathy, L. Athanasius, R. Velraj, and R. V. Seeniraj, “Experimental investigation  
 566 and numerical simulation analysis on the thermal performance of a building roof  
 567 incorporating phase change material (PCM) for thermal management,” *Applied Thermal*  
 568 *Engineering*, vol. 28, no. 5, pp. 556–565, Apr. 2008.  
 569  
 570 [10] H. F. Castleton, V. Stovin, S. B. M. Beck, and J. B. Davison, “Green roofs; building  
 571 energy savings and the potential for retrofit,” *Energy and Buildings*, vol. 42, no. 10, pp.  
 572 1582–1591, 2010.  
 573  
 574 [11] M. Çelebi and H. P. Liu, “Before and after retrofit – response of a building during  
 575 ambient and strong motions,” *Journal of Wind Engineering and Industrial*  
 576 *Aerodynamics*, vol. 77, no. 0, pp. 259–268.  
 577  
 578 [12] S. R. Gaffin, M. Imhoff, C. Rosenzweig, R. Khanbilvardi, A. Pasqualini, A. Y. Y. Kong,  
 579 D. Grillo, A. Freed, D. Hillel, and E. Hartung, “Bright is the new black—multi-year  
 580 performance of high-albedo roofs in an urban climate,” *Environ. Res. Lett.*, vol. 7, no. 1,  
 581 p. 014029, Mar. 2012.  
 582  
 583 [13] R. VanCuren, “The radiative forcing benefits of ‘cool roof’ construction in California:  
 584 quantifying the climate impacts of building albedo modification,” *Climatic Change*, vol.  
 585 112, no. 3, pp. 1071–1083, Sep. 2011.  
 586  
 587 [14] P. Mukhopadhyaya, M. T. Bomberg, M. K. Kumaran, M. Drouin, J. C. Lackey, D. van  
 588 Reenen, and N. Normandin, “Long-term thermal resistance of polyisocyanurate foam  
 589 insulation with gas barrier,” pp. 1–10, 2004.



- 590  
591 [15] R. T. A. Prado and F. L. Ferreira, "Measurement of albedo and analysis of its influence  
592 the surface temperature of building roof materials," *Building and Environment*, vol. 37,  
593 no. 4, pp. 295–300, Apr. 2005.  
594
- 595 [16] H. Akbari, A. Berhe, R. Levinson, S. Graveline, K. Foley, A. Delgado, and R. Paroli,  
596 "Aging and Weathering of Cool Roofing Membranes," *eScholarship, University of*  
597 *California*, pp. 1–15, Aug. 2005.  
598
- 599 [17] M. Bomberg, "A model of aging for gas-filled cellular plastics," *Journal of cellular*  
600 *plastics*, vol. 24, no. 4, pp. 327–347, 1988.  
601
- 602 [18] M. Bomberg and D. A. Brandreth, *Evaluation of longterm thermal resistance of gas-*  
603 *filled foams: state of the art*, 2nd ed. Philadelphia: American Society for Testing and  
604 Materials, 1990, pp. 156–173.  
605
- 606 [19] S. K. Meyn and T. R. Oke, "Heat fluxes through roofs and their relevance to estimates of  
607 urban heat storage," *Energy and Buildings*, vol. 41, no. 7, pp. 745–752, 2009.  
608
- 609 [20] F. Ingelrest, G. Barrenetxea, G. Schaefer, M. Vetterli, O. Couach, and M. Parlange,  
610 "SensorScope," *ACM Trans. Sen. Netw.*, vol. 6, no. 2, pp. 1–32, Feb. 2010.  
611
- 612 [21] Z. Wang, E. Bou-Zeid, and J. A. Smith, "A coupled energy transport and hydrological  
613 model for urban canopies evaluated using a wireless sensor network," *Quarterly Journal*  
614 *of the Royal Meteorological Society*, vol. 139, no. 675, pp. 1643–1657, 2013.  
615
- 616 [22] A. Desjarlais, T. Petrie, W. Miller, R. Gillenwater, and D. Roodvoets, "Evaluating the  
617 energy performance of ballasted roof systems," presented at the 3rd International  
618 Building Physics Conference, Montreal, 2006.  
619
- 620 [23] C. P. Hedlin, "Calculation of Thermal Conductance Based on Measurements of Heat  
621 Flow Rates in a Flat Roof Using Heat Flux Transducer," American Society for Testing  
622 and Materials, Philadelphia, 1351, Feb. 1985.  
623
- 624 [24] D. Li and E. Bou-Zeid, "Synergistic interactions between urban heat islands and heat  
625 waves: the impact in cities is larger than the sum of its parts," *Journal of Applied*  
626 *Meteorology and Climatology*, vol. 52, no. 9, pp. 2051–2064, Oct. 2013.  
627  
628

628 Highlights:

629

630 • Spatial (vertical) and temporal variation in heat flux observed over multiple roofs

631

632 • Albedo plays a dominant role in reducing the heat transfer in summer months

633

634 • Doubling insulation thickness halves heat transfer in winter months

635

636 • Wintertime penalty of white roofs negligible compared to summer savings

637

638 • White roofs with high R-values recommended to North Eastern U.S.

639

640

641

---

# Princeton Plasma Physics Laboratory Office of Reports and Publications

Managed by  
Princeton University

under contract with the  
U.S. Department of Energy  
(DE-AC02-09CH11466)

---

P.O. Box 451, Princeton, NJ 08543  
Phone: 609-243-2245  
Fax: 609-243-2751

E-mail: [publications@pppl.gov](mailto:publications@pppl.gov)

Website: <http://www.pppl.gov>